Issues related to velocity structure estimation in small coastal sedimentary plains - Case of Tottori plain facing the Sea of Japan

Takao Kagawa (kagawa@cv.tottori-u.ac.jp)
Tottori Daigaku Daigakuin Kogaku Kenkyuka Kogakubu https://orcid.org/0000-0001-6557-4855
Tatsuya Noguchi
Tottori Daigaku Daigakuin Kogaku Kenkyuka Kogakubu

Express Letter

Keywords: Small coastal plain, Predominant period, Velocity structure, Diffuse wave field theory, Tottori plain

Posted Date: October 11th, 2021

DOI: https://doi.org/10.21203/rs.3.rs-951437/v1

Title page:

Title: Issues related to velocity structure estimation in small coastal sedimentary plains - Case of Tottori plain facing the Sea of Japan -

Author #1: Takao Kagawa, Tottori University, Faculty of Engineering, 4-101 Koyamacho-Minami, Tottori, Japan, kagawa@tottori-u.ac.jp

Author #2: Tatsuya Noguchi, Tottori University, Faculty of Engineering, 4-101 Koyamacho-Minami, Tottori, Japan, noguchit@tottori-u.ac.jp

Corresponding author: Takao Kagawa

(go to new page)

Abstract

Issues of predominant period of ground motion and derived underground velocity structure model were investigated in the coastal plains affected by the soft sedimentary layer after the last ice age. Specifically, it is found that two predominant periods due to the shallow soft sediments and deep sedimentary layers over the seismic bedrock created by the tectonic movement after the quaternary period are close in a small plain such as the Tottori Plain, Japan as an example. It was shown by the analysis of underground velocity structure derived from H/V spectrum ratio of earthquake ground motions with the diffuse wave field theory. It is feared that the interaction of close predominant periods due to the different layer boundaries with high contrast may amplify the seismic motion in the period range that affects building structures in the small plains in coastal area.

Keywords

Small coastal plain, Predominant period, Velocity structure, Diffuse wave field theory, Tottori plain

Main Text

Introduction

In the coastal plains, a soft layer deposited by Holocene transgression from the end of the last ice age generate a notable predominant period, generally shorter than 1 sec., in contrast with the engineering bedrock (Predominant Period 1). On the other hand, the plains and basins in Japan are affected by tectonic movements during the Quaternary period and have thick sedimentary layers in the area relatively subsided from the surrounding mountains. Another predominant period is formed by the contrast between the sedimentary layers and the seismic bedrock (Predominant Period 2). It is well known that large sedimentary plains such as the Kanto, Nobi, and Osaka plains have thick sedimentary layers over the seismic bedrock, and the Predominant Periods 2 are several seconds. However, in small plains such as the Tottori plain, Japan (Fig. 1), the sediment on the seismic bedrock is thinner than in the large plains, and in places where the Predominant Period 1 is long, it might be close to the Predominant Period 2. Therefore, the diffuse wave field theory (Kawase et al., 2011) was applied to H/V spectrum ratio of earthquake ground motions at strong ground motion observation site

43 in the Tottori plain to estimate the velocity structure model, and after verifying its
44 validity, contribution of each layer boundary to the predominant period was examined.
45
46 **Estimation of Velocity Structure from H/V of Earthquake Ground Motion**
47 The TTR002 site of K-NET (National Research Institute for Earth Science and Disaster
48 Resilience, 2019) is targeted as a strong motion observation site in the Tottori plain.
49 Eight records with an epicentral distance of 100 km or less and a maximum acceleration
50 of 10 to 100 cm/s^2 were selected, that are not affected by surface waves and non-linear
51 ground responses. The records are the 2000 western Tottori prefecture earthquake
52 (M_J7.3), the 2016 Central Tottori prefecture earthquake (M_J6.6), and other six
53 earthquakes with M_J 3.2 to 5.4. Locations of the epicenters are shown in Fig. 1. The
54 averaged H/V spectral ratio was obtained from the three component observation records
55 for 40.96 seconds mainly contain the S wave portion. Vector sum of NS and EW
56 channels is used to evaluate horizontal component as to match the diffuse wave field
57 theory.
58 The results are shown as gray lines in Fig. 2(a). The spectrum was smoothed by the

59 filter proposed by Konno and Ohmachi (1995) that provides the same smoothing over
60 the entire frequency range in logarithmic axis. The result has remarkable peak around 1
61 sec., and the spectra are stable for all the earthquakes. As a reference, H/V spectrum
62 ratio of microtremor measurement performed near the observation point is shown in
63 Fig. 2(b). Both shapes are similar, but the levels are slightly different. The horizontal
64 motion of the microtremor is not calculated by vector sum but synergistic average,
65 however, the H/V of earthquake ground motion is larger even the difference is taken
66 into condition. In addition, the maximum peak appears around 0.7 to 0.8 sec., which
67 seems to be slightly shorter than the peak of earthquake ground motion.
68 The underground velocity structure model was estimated so that the calculated H/V by
69 the diffuse wave field theory (Kawase et al, 2011) agrees well with the observed H/V
70 spectrum of the earthquake ground motion. Simulated annealing (SA, Ingber, 1989) are
71 applied to search the proper model. Out of the 200 initial models generated within the
72 search range by random numbers, 20 models with a small difference from the
73 observation are survived. Around the parameters of 20 models, new parameters for next
74 step are generated with random numbers in the range corresponding to the temperature

75 at the step. In addition, a hybrid heuristic search was performed by considering the
76 genetic algorithm (GA, Holland, 1975) as allowing crossing of parameters in each layer.
77
78 **Estimated Velocity Structure**
79 Fig. 2(c) and (d) shows the results of 21 cases performed with different initial random
80 numbers in gray lines, the optimum solution in bold line, and the search range in thin
81 solid lines, for S wave velocity and attenuation as target physical parameters. The other
82 parameters, P wave velocity and density, are evaluated from the S wave velocity using
83 empirical formulae. Kitsunezaki et al. (1990) is used to evaluate P wave velocity from S
84 wav velocity, and Gardner et al. (1974) is used to estimate density from P wave
85 velocity. A 200-step SA search was carried out while lowering temperature so that the
86 integrated area of difference between observation and calculation in the spectral figure
87 is minimized. Fig. 2(a) shows the H/V calculated from the optimum solution (Fig. 2(e))
88 in black line together with the observation in gray line. The shape of calculated H/V
89 around the predominant period 1 sec. seems to be composed of two small peaks.
90 Independently, microtremor array observation was conducted around the observation

site (Noguchi et al, 2003; Ishida et al., 2013). Fig. 3 shows the Rayleigh wave phase velocity of fundamental mode by the velocity structure model obtained here with the observed data. Their consistency suggests the validity of the estimated velocity structure model.

Discussion

It is examined which layer boundary corresponds to the predominant period of the observed H/V from earthquake ground motion. First, we tried to make the base layer shallower by deleting layers of the model in order from the deepest part. The result is shown in Fig. 4. The "Upper 9 Layers" on the upper left is almost the same as the original, and there might be almost no effect even if the base layer of Vs = 3.2 km/s is set to Vs = 2.715 km/s. According to other surveys, the depth of the bedrock in the Tottori Plain is about 300 m (Noguchi et al, 2003), and the corresponding "Upper 6 Layers" model can almost explain outline of observed H/V. The explanation of the observation becomes worse as deleting the deep layers, but the tendency mentioned above does not change until "Upper 6 Layers" model. For the first time in the "Upper 5

Layers" model, the predominance of period 1 sec. collapsed. It increases around period 0.7 to 0.8 sec. although it is small. It is considered that this corresponds to the peak seen in microtremor H/V shown in the left panel of Fig. 3. Since the peak with a period of 0.7 to 0.8 sec. disappears from "Upper 4 Layers" and only 0.2 seconds or less is predominant, the peak observed in microtremor is represented by the sediments of about 30 m thickness to the 4th layer as engineering bedrock with Vs = 0.322.

Fig. 5 shows the results of calculating the H/V spectrum by combining the surface layers in order from the shallow layer and obtaining the average S wave velocity of the combined layer in the same way as AVS30 evaluation (Joyner and Fumal, 1984). P wave velocity and density of the combined layer were reset from the S wave velocity using empirical formulae, and the attenuation was set by the weighted average according to layer thickness. On the Top left panel of Fig. 5, the surface layer and the second layer are combined, “2 Shallow Layers Combined”, and it is suggested that the predominance of 0.1 to 0.2 sec. is affected by the first layer. This is consistent with the results seen in Fig. 4. Combined from surface to the third layer, “3 Shallow Layers Combined”, the predominance of 0.3 sec. or less disappeared. This period range might

123 be affected by the surface layers shallower than about 14 m. After “5 Shallow Layers
124 Combined”, about 0.8 seconds of the two peaks that perform predominance around 1
125 sec. of the calculated H/V became smaller. As seen in Fig. 4, this period band is
126 influenced by shallower sediments over engineering bedrock. This tendency is same for
127 “Shallow 6 Layers Combined”, however, after “7 Shallow Layers Combined”, the peak
128 shifts to longer period. Therefore, it is suggested that the peak with a period around 1
129 sec. seen H/V of earthquake ground motion is generated at the boundary with S wave
130 velocity about 1.0 km/s layer at a depth around 90 m. The depth of bedrock expected at
131 target site in Tottori plain about 300 m corresponds to the model “7 Shallow Layers
132 Combined”. The peak is calculated as longer than 2 seconds due to the surface
133 sedimentary layers, and it can be seen slightly in the observed H/V. However, in the
134 calculation here, peaks are emphasized by increasing the contrast between the average S
135 wave velocity combined with the surface layers and that of the bedrock. It is considered
136 that the influence of deeper layers than 300 m on amplification is not large enough.
137 Thus, overlap of two remarkable peaks due to the very surface layer up to the
138 engineering bedrock and the deeper sedimentary layer over seismic bedrock suggests

that a particularly large amplitude predominance was formed around the period 1 sec. at the target site. In large-scale plains, the predominant periods due to the boundary between those two high contrast boundaries are separated, so they do not interact with each other. However, in the small sedimentary plain formed in the coastal area, the phenomenon introduced in this study is highly concern, so it is considered as one of the issues to be addressed in earthquake disaster prevention. Even if the target place is small plane or basin but in mountainous area, the results of this study are not directly applied because the place is not affected by shallow soft sediments formed from regression or transgression effects. The situations depend on the geological history of target places.

Conclusion

The underground velocity structure was estimated by applying the diffuse wave field theory (Kawase et.al, 2011) to the seismic observation records in the Tottori Plain, and the layer boundary showing the predominant period was examined. The conclusions derive from the study are as follows.

1) In the coastal plains, a soft layer accompanies the transgression from the regression

155 of the last ice age to the Holocene is deposited, and a clear predominant period can be
156 seen in contrast with the engineering bedrock.
157 2) The plains of Japan are affected by tectonic movements after the beginning of th
158 Quaternary, and another predominant period is formed by the contrast of the deeper
159 layer boundary to the seismic bedrock.
160 3) In large plains, the predominant period caused by 2) is significantly longer than that
161 by 1), and their effects appear in different period ranges.
162 4) In a small plain, it is feared that the overlap of these two predominant periods will
163 increase the amplification of earthquake ground motion by the sedimentary layers.
164 5) Since the same phenomenon is suggested in the small sedimentary plain formed in
165 the coastal area, it might be one of the issues to be considered in earthquake disaster
166 prevention.
167 There are many plains of the same scale on the coast of the Sea of Japan that have the
168 same geological history as the Tottori Plain, and the conclusions here will be useful in
169 considering future earthquake disaster prevention in those areas.
170

171 **Figures and legends**

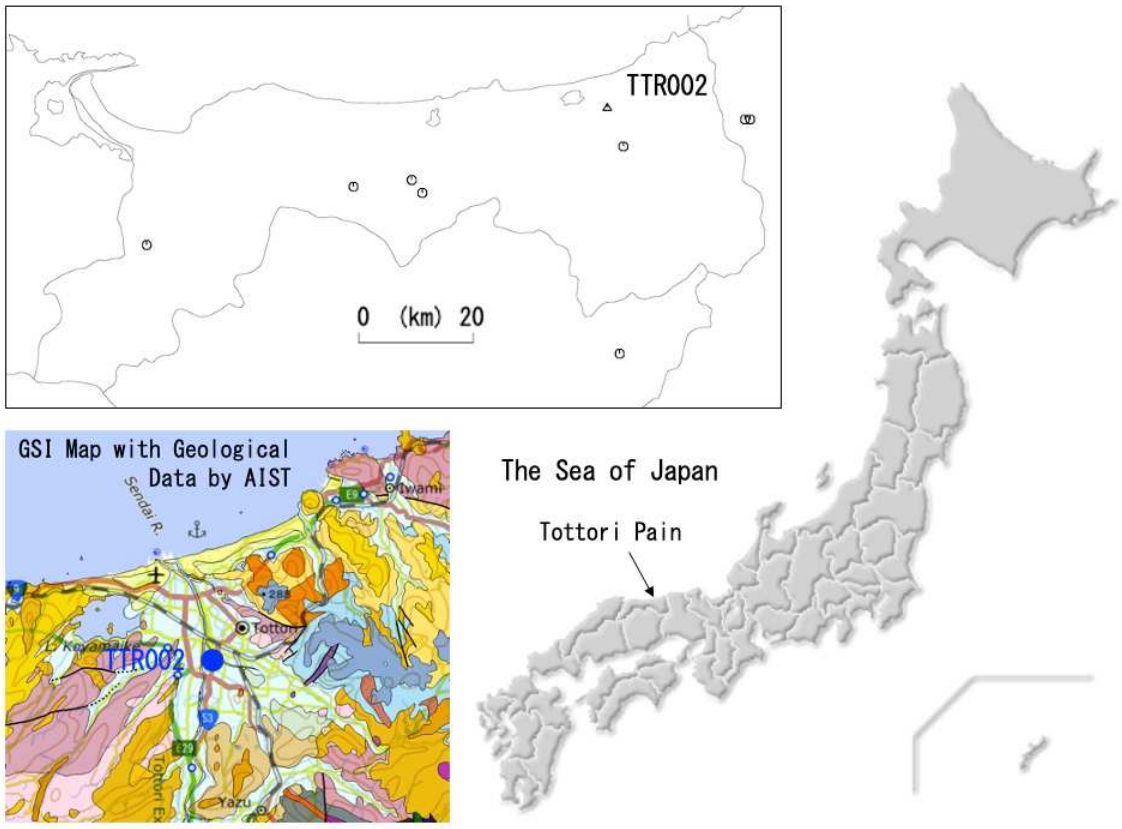

172

173 Fig. 1

174 Location of Tottori plain and target site TTR002 with epicenter distribution of the

175 earthquakes used in the study

176 Geological map in left bottom panel shows the area of Tottori plain (lime green).

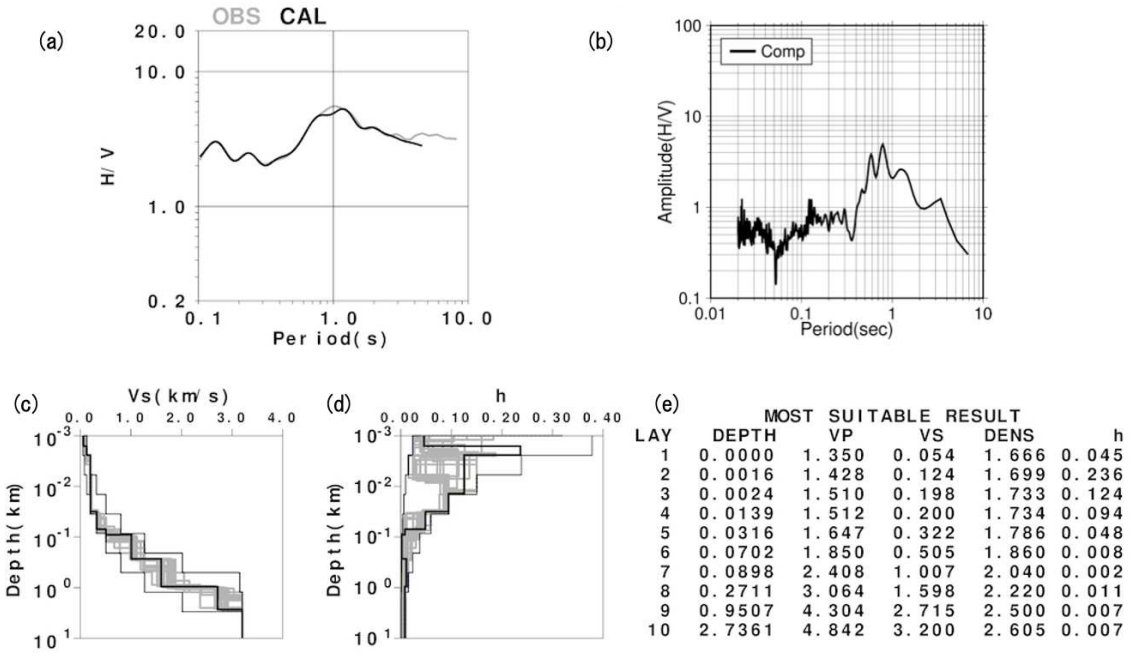

Fig. 2 Observed and calculated H/V of earthquake ground motion with estimated underground structures

(a) Observed (gray) and calculated (black) H/V of earthquake ground motion at TTR002 site

(b) Observed microtremor H/V near the TTR002 site

(c) S wave velocity model with the results of 21 cases performed with different initial random numbers (gray lines), the optimum solution (bold line) from which black line of (a) is calculated, and the search range (thin solid lines)

(d) Same as (c) but for attenuation model

(e) Detailed parameters of the optimum solution in (c) and (d)

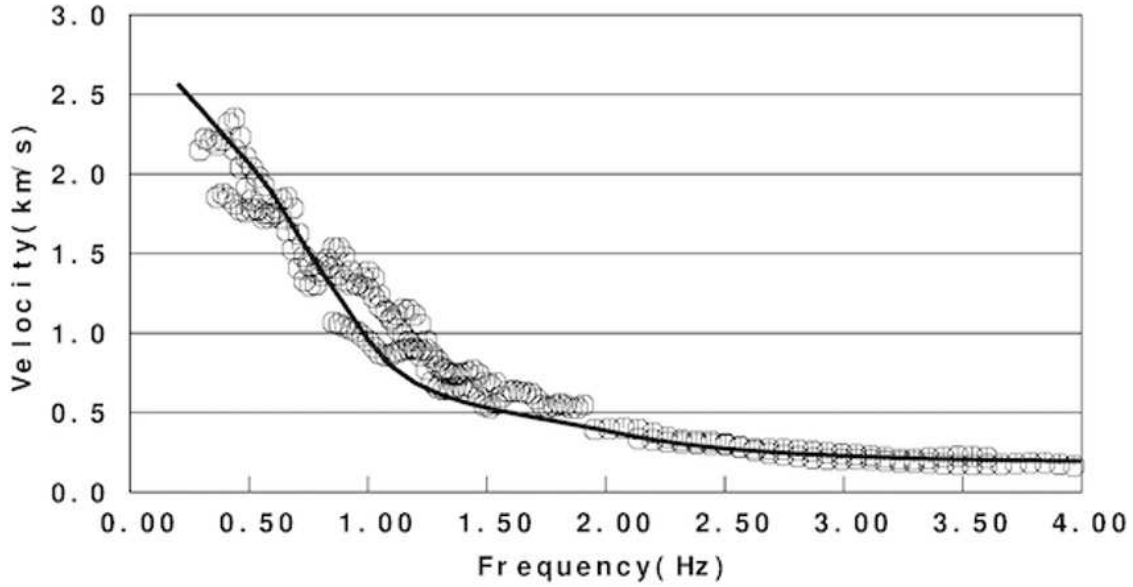

188

189 Fig. 3

190 Rayleigh wave dispersion curve calculated from the model shown in Fig. 2(e) (bold

191 line) and phase velocities from microtremor array observation

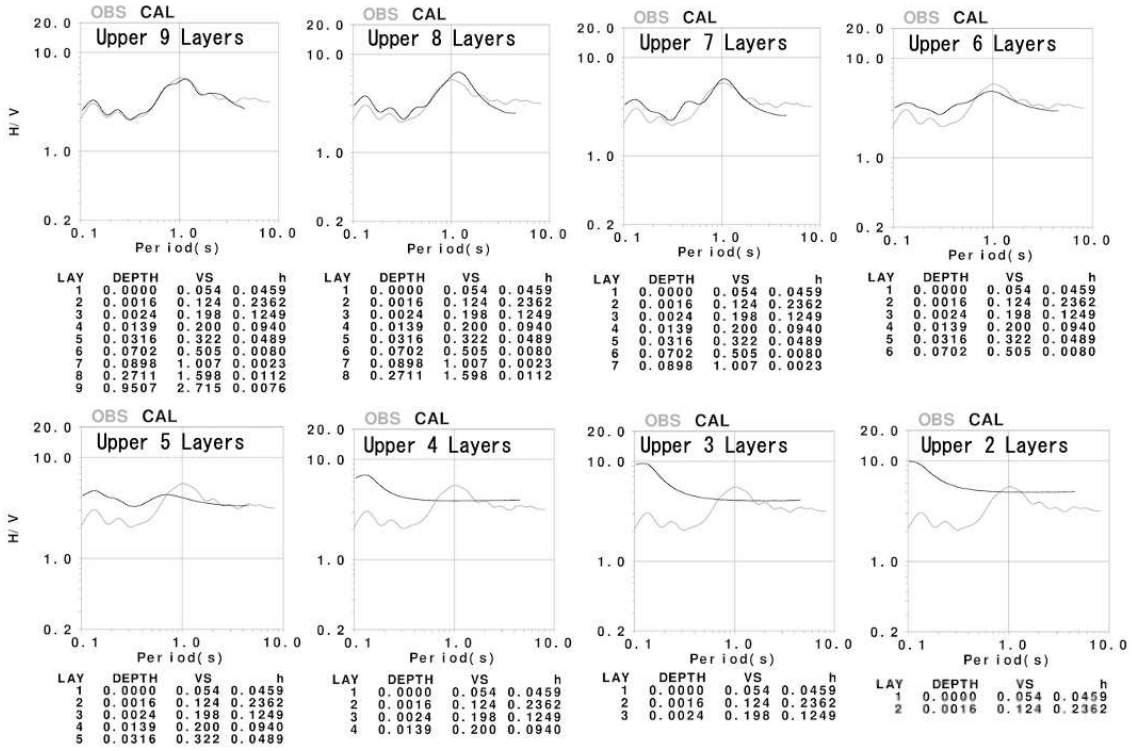

192

Fig. 4

Calculated H/V of earthquake ground motion with making the base layer shallower by deleting layers of the model in order from the deepest part

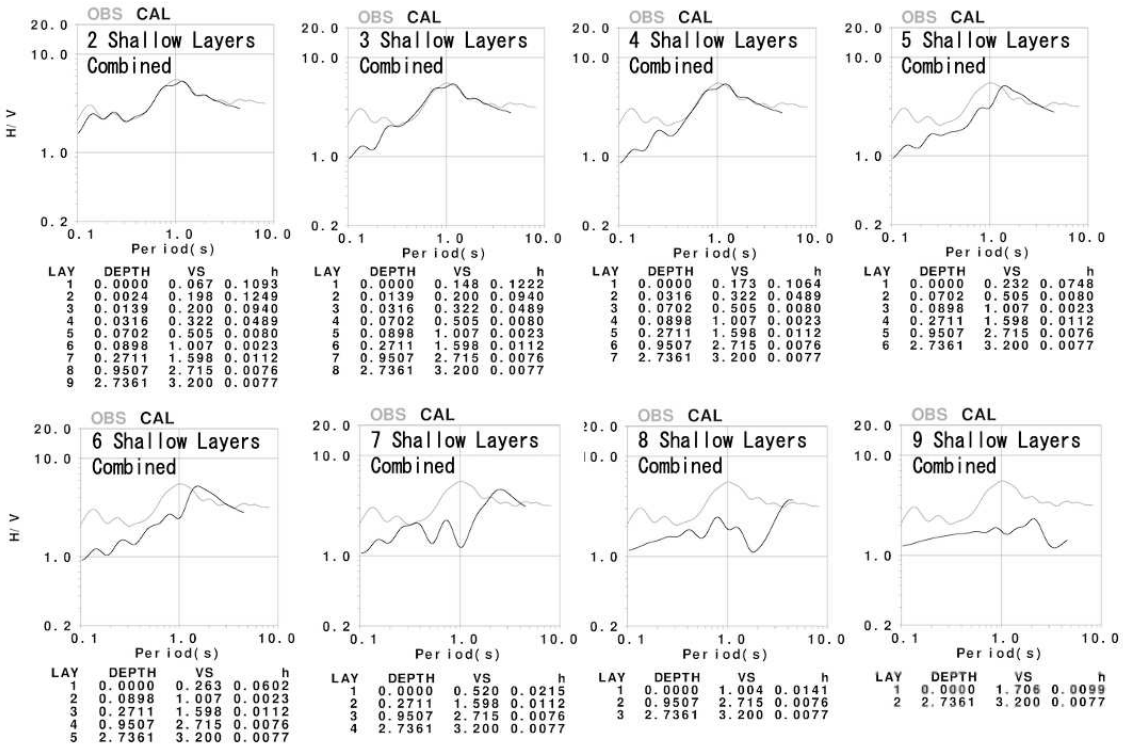

Fig. 5

Calculated H/V spectrum by combining the surface layers in order from the shallow layer with evaluated average S wave velocity of the combined layer

Declarations

The authors *must* provide the following sections under the heading "Declarations".

Ethics approval and consent to participate

Not applicable.

Consent for publication

Not applicable.

List of abbreviations

H/V	Horizontal components over Vertical component
K-NET	Kyoshin (Strong Motion in Japanese)-NETwork maintained by National Research Institute for Earth Science and Disaster Resilience

Availability of data and materials

Strong motion data at K-NET TTR002 are available from National Research Institute for Earth Science and Disaster Resilience (NIED) at http://www.kyoshin.bosai.go.jp (last accessed September 2021). Microtremor observation data conducted around TTR002 site are available on contacting the authors.

Competing interests

The authors declare that they have no competing interests.

Funding

This study was partially supported by Ministry of Education, Culture, Sports, Science and Technology (MEXT) of Japan, under its The Second Earthquake and Volcano Hazards Observation and Research Program (Earthquake and Volcano Hazard Reduction Research).

Authors' contributions

TK made analysis of strong ground motion records and TN conducted microtremor observations and integrated the results. After discussion among authors, TK drafted the manuscript. All authors read and approved the final manuscript.

Acknowledgements

The authors appreciate Mr. Isamu Nishimura who made a fine figure of microtremor H/V around the target site.

Authors' information

Tottori University, Faculty of Engineering, 4-101 Koyamacho-Minami,

Tottori, Japan

Takao Kagawa & Tatsuya Noguchi

Endnotes

None

References

Gardner G H F, Gardner L W, Gregory A R (1974) Formation velocity and density – the diafnostic basics for stratigraphic traps, Geophysics, 39(6), 759-918

Holland J H (1975) Adaptation in natural and artificial systems, The Univ. Michigan Press

Ingber L (1989) Very fast simulated annealing, Math. Comput. Modeling, 12, 967-973

Ishida Y, Noguchi T, Kagawa T (2013) Modeling 3-D subsurface structure for strong ground motion estimation in the Tottori plain, Journal of Japan Society of Civil Engineering, A1, 69(4), I_821-I_828 (in Japanese with English abstract)

Joyner W and Fumal T (1984) Use of measured shear-wave velocity for predicting geologic site effects on strong ground motion, Proc. 8th World Conf. on Earthq. Eng.,

777-783

Kawase H, Sánchez-Sesma F J, Matsushima S (2011) The optimal use of horizontal-to-vertical spectral ratios of earthquake motions for velocity inversions based on diffuse-field theory for plane waves, Bull. Seism. Soc. Am., 101(5), 2001-2014

Kitsunezaki C, Goto N, Kobayashi Y, Ikawa T, Horike M, Saito T, Kuroda T, Yamane K, Okuzumi K (1990) Estimation of P- and S- wave velocities in deep soil deposits for evaluating ground vibrations in earthquake", J. Natural Disaster Science, 9(3), 1-17. (in Japanese with English abstract)

Konno K, Ohmachi T (1995) A smoothing function suitable for estimation of amplification factor of the surface ground from microtremor and its application, Journal of Japan Society of Civil Engineering, 524(I- 33), 247-259. (in Japanese with English abstract)

National Research Institute for Earth Science and Disaster Resilience (2019), NIED K-NET, KiK-net, National Research Institute for Earth Science and Disaster Resilience, doi:10.17598/NIED.0004

Noguchi T, Nishida R, Okamoto T, Hirasawa T (2003) Determination of the subsurface

267 structure of Tottori plain using seismic explosion, microtremor, and gravity exploration,

268 Proc. Earthquake Engineering Symposium, Japan Society of Civil Engineering, 23, #

269 197. (in Japanese with English abstract)

270

Supplementary Files

This is a list of supplementary files associated with this preprint. Click to download.

- GraphicalAbstract.png